Broad polymorphism of fatty acids with amino organo silane counter ions, towards novel templates

Cédric Gaillard , Bruno, Novales, François Jérôme and Jean-Paul Douliez*.

JPD and BN: UR 1268 Biopolymères Interactions Assemblages, INRA, BIA/ISD, rue de la Géraudière, 44316 Nantes, France, FJ: Laboratoire de Catalyse en Chimie Organique, CNRS/Université de Poitiers, 40 av. du recteur Pineau, 86022 Poitiers, France. CG: UR 1268 Biopolymères Interactions Assemblages, INRA, BIA/plateforme microscopie BIBS RIO, rue de la Géraudière, 44316 Nantes, France

Supporting information :

1) Phase contrast microscopy:

Observations were made at room temperature at 20x magnification using an optical microscope in the phase contrast mode (Nikon Eclipse E-400, Tokyo, Japan) equipped with a 3-CCD JVC camera allowing digital images (768 x 512 pixels) to be collected. A drop of the lipid dispersion (about 20µL) was deposited on the glass slide surface (76x26x1.1 mm, RS France) and covered with a cover slide (22x22 mm, Menzel-Glaser, Germany). The glass slides were previously cleaned with ethanol and acetone.

The micrograph for a dispersion of vesicles made of the APTES salt of myristic acid in pure water is shown here-after, the scale bar corresponds to 10µ.

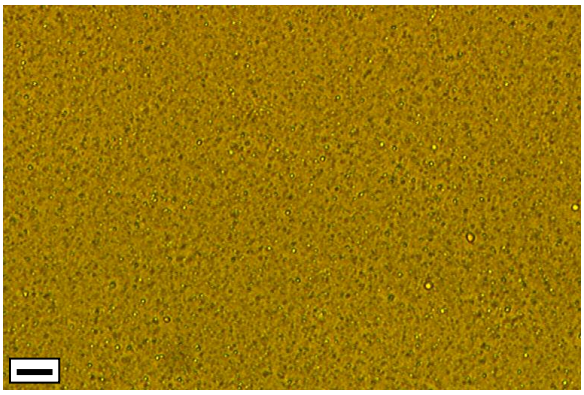

2) Differential scanning calorimetry

Differential scanning calorimetry for a 1% sample of the APTES salt of myristic acid in water. Experiments were performed on a MicroCal DSC apparatus. The amount of 1.3 mL of the lipid solution was accurately poured in the cell. The scan was recorded between 10 and 80°C at 1°C/min. The DSC trace from the second heating step is shown for a 1% gel and shows the broad phase transition of the melting of the gel at around 35°C.

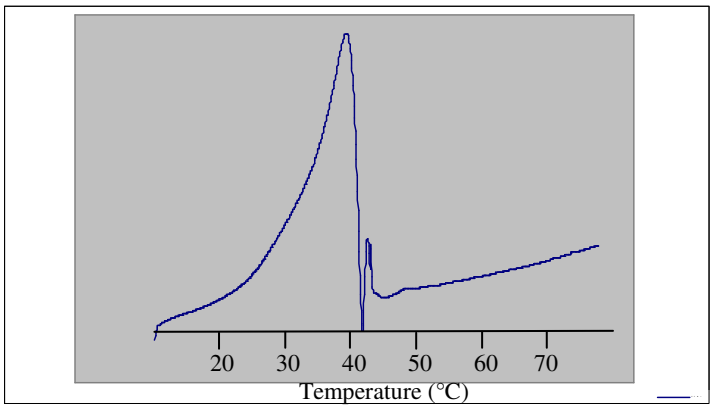

3) Deuterium solid state NMR data

Deuterium solid state NMR experiments were performed at several temperatures from 20 to 70°C on a 400MHz Bruker spectrometer operating at 61MHz for deuterium using a static double channel probe. The sample coil of the probe was adapted to load a 7mm rotor such as those used for magic angle spinning probes equipped with a stretched stator. Typically, lipid dispersions were previously heated to 70°C and a volume of *ca.* 700µL transferred into the rotor which was sealed and then end-capped. A Hahn quadrupolar echo sequence [1] was used with an inter pulse delay of 40µs. Eight k points in 1k accumulations (every 2s) were done with a 90 deg pulse and spectral width of 8µs and 250 kHz, respectively. Free induction decay signal were zero-filled to 16k points prior to Fourier transform after a broad line exponential multiplication of 200Hz. Deuterated materials were from Eurisotop, CEA, Saclay, France.

For deuterium spectroscopy, the general theory for lipid systems can be found in the literature [1, 2]. Briefly, the deuterium NMR signal is composed of doublets with a splitting, $\Delta\nu$, which depends on the orientation of the C-D bond with respect to the magnetic field. In an

anisotropic but *disoriented* medium, all the orientations are allowed and these doublets are superimposed to form a powder spectrum having two main peaks with an increased intensity corresponding to the 90 deg orientation, separated by $\Delta\nu_{90}$. The edge of the spectrum corresponds to the 0 deg orientation, with a splitting $\Delta\nu_0$ equal to twice $\Delta\nu_{90}$. In the case of perdeuterated systems, the spectrum is composed by the superimposition of signals from each labeled position. In all spectra, an isotropic signal can be observed and is attributed to the natural abundance deuterated water since non depleted deuterated water was used for preparing the samples.

In the case of myr-APTES vesicles at pH 9.5 at room temperature (top spectrum), the spectrum is characteristic of fatty acids embedded in a fluid phase [1]. It is composed of superimposed signals corresponding to the labeled positions of perdeuterated myristic acid with quadrupolar splittings between 3 kHz (terminal methyl group) and 37 kHz (other positions). Typically, 6 positions can be clearly resolved. The shoulders are clearly missing showing that the vesicles self orient in the magnetic field in a prolate form. Similar spectra have been recorded for fatty acid forming vesicles in a fluid state [3, 4]. For the vesicles at pH 6 (middle spectrum), the spectrum is composed of two main components, the first with a splitting of 55 kHz and the other one of 11 kHz. This feature is characteristic of fatty acids embedded in a gel phase [1, 3].

In the case of the gel of myr-APTES (at basic pH), the spectrum (bottom spectrum) is also composed of two main components, but with larger splittings, the first one of 125 kHz and the other one of 37 kHz. This feature is characteristic of fatty acids embedded in crystals [1, 3].

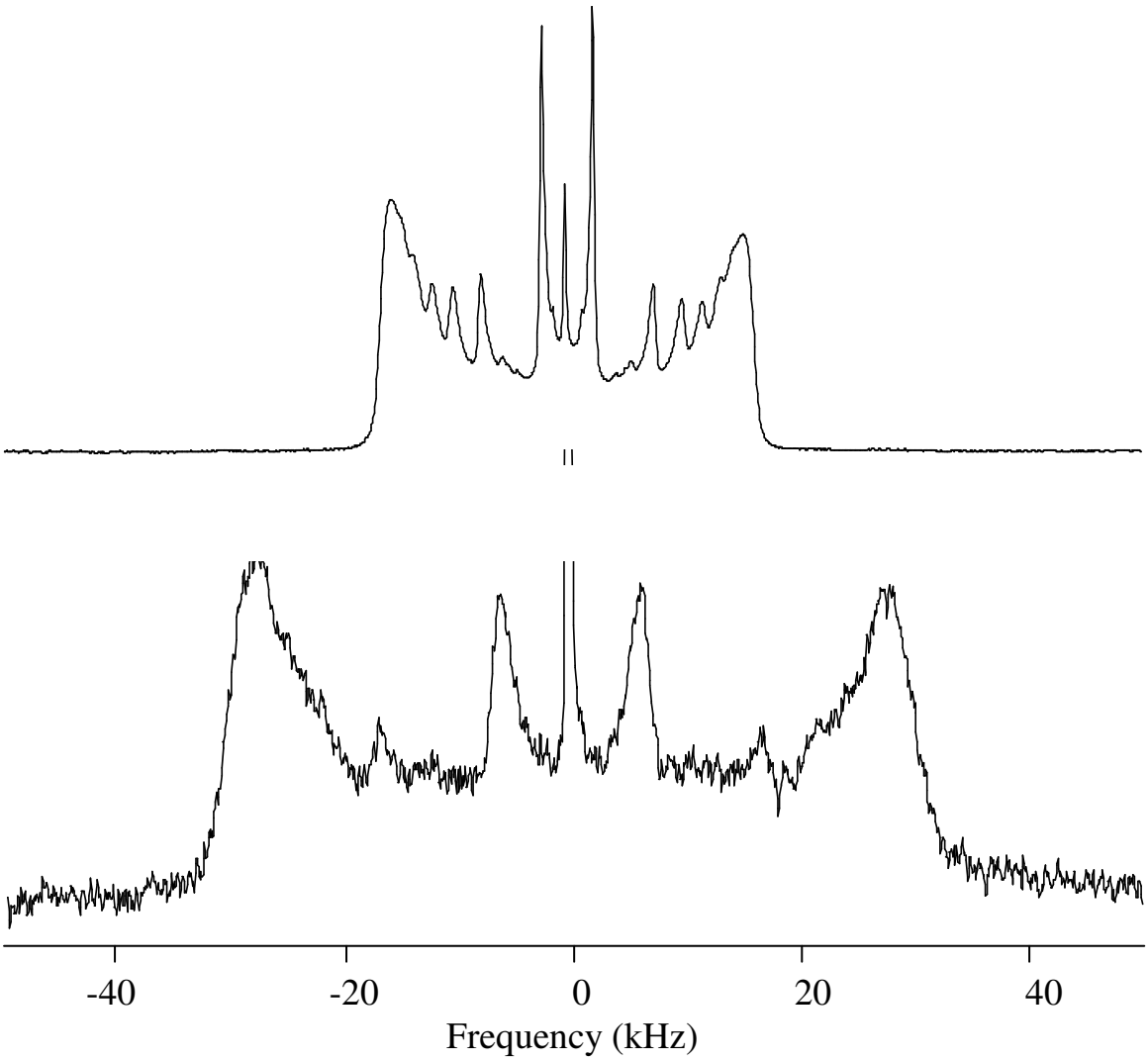
-40
-20
0
20
40
Frequency (kHz)

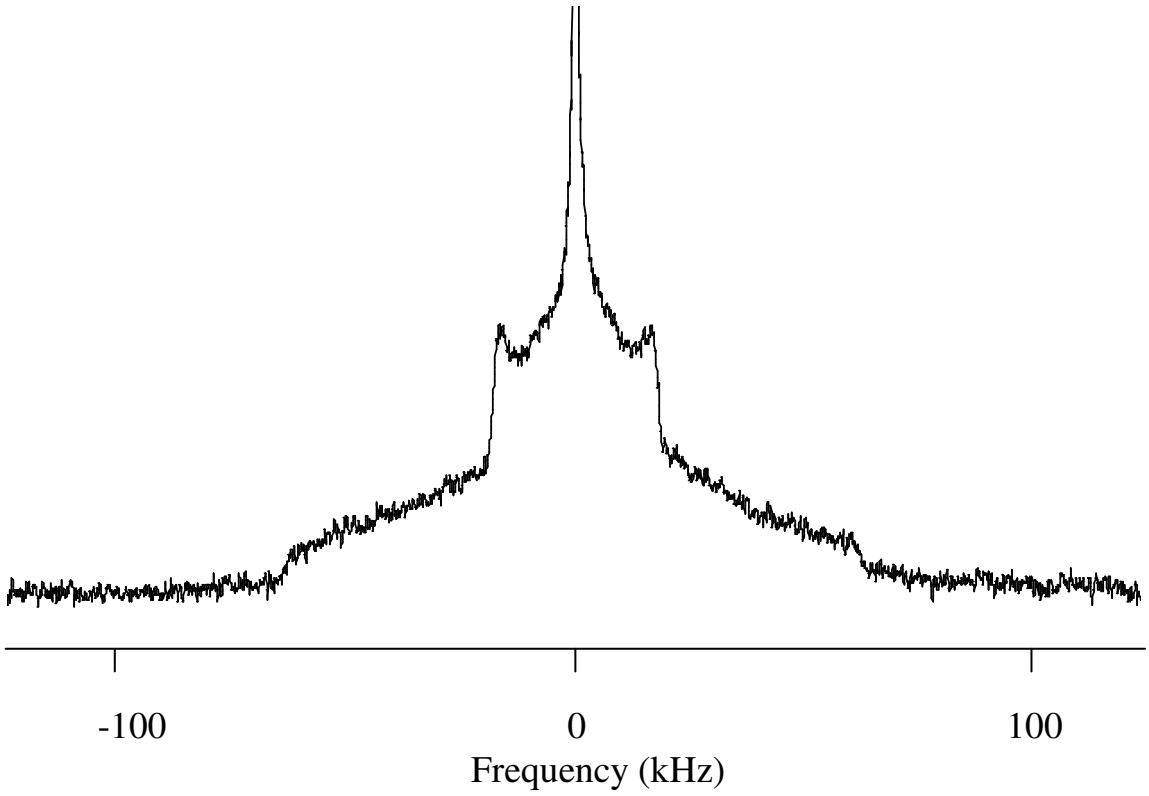
-100
0
100
Frequency (kHz)

4) Additional SEM images on Myr/APTES gels

50 µl of an aqueous dispersion of each specimen was deposited on a copper SEM stub and air-dried. The samples were then sputter coated with a fine gold layer (approx 100-200 Å) before obtaining the micrographs. The samples were observed in a JEOL JSM 6300 scanning electron microscope (JEOL, Tokyo, Japan) using low-voltage conditions. The authors wish to thank Mr. Paul Pilet, from the Research Center on Materials with Biological Interest from Nantes, for his precious help and fruitful discussion in scanning electron microscopy.

Scale bar 1µ

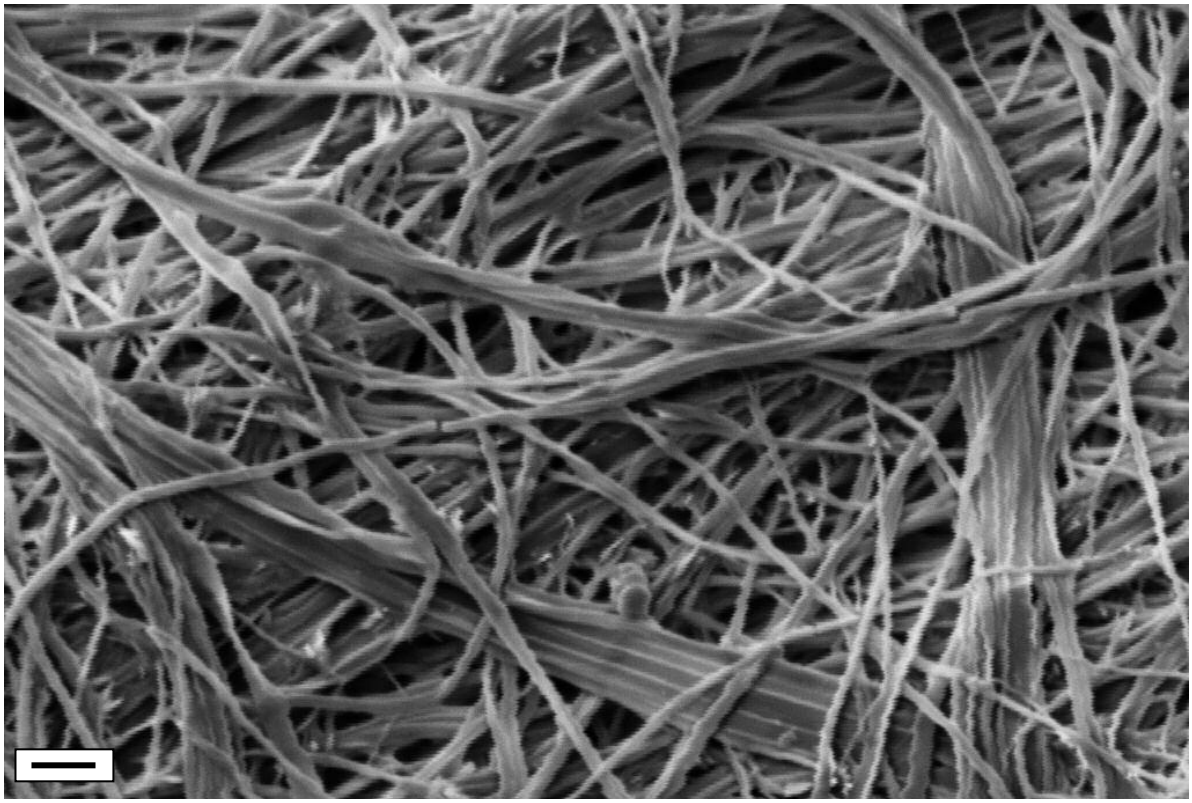

5) Preliminary small angle neutron scattering data:

Small-angle neutron scattering (SANS) experiments were performed at Laboratoire Léon-Brillouin (laboratoire mixte CEA—CNRS, Saclay, France) on spectrometer PAXY. The neutron beam was collimated by appropriately chosen neutron guides and circular apertures, with a beam diameter at the sample of 7.6 mm. The neutron wavelength was set to 0.4 or 0.8 nm with a mechanical velocity selector ($\Delta\lambda/\lambda \approx 0.1$), the 2D detector (128x128 pixels, pixel size 5x5 mm^2) being positioned at 1.4 or 6.7 m, respectively. The scattering wave vector, q, typically ranges from 0.06 to 5 nm^{-1}, with a significant overlap between the two configurations. The samples, prepared with deuterated water (Eurisotop), were held in flat quartz cells with a 2 mm optical path and temperature-controlled by a circulating fluid to within ±0.2°C. The azimuthally-averaged spectra were corrected for solvent, cell and incoherent scattering, as well as for background noise.

The general theory for fitting the SANS data can be found in the literature [5]. Briefly, the scattered intensity can be described as the product of a *structure factor S(Q)*, characteristic of the correlations between objects, by a *form factor P(Q)*, describing the shape of the objects. The form factor of a completely filled, spherical object of radius R (a model appropriate for spherical micelles) is known to be given by:

$$P_{sph}(Q) = 9 \cdot \left[\frac{\sin QR - QR\cos QR}{(QR)^3} \right]^2$$

In the case of the gel at room temperature (curve 1), the diffusion pattern exhibit a slope of Q^{-4} at low Q indicative of supramolecular objects having a flat solid surface of large thickness characteristic of fatty acid crystals. The peak at $2\pi/Q = 0.18$ corresponds to a characteristic distance of 35 Å and stands for the thickness of each crystals stacked together. This peak disappears when one uses perdeuterated myristic acid (not shown). Such a thickness is consistent of a bilayer arrangement since it corresponds to about twice that of the fatty acid chain length in its extended conformation. For the solution at high temperature (60°C, curve

2), the pattern is characteristic of micelles the diameter of which could be estimated to be 40 Å.

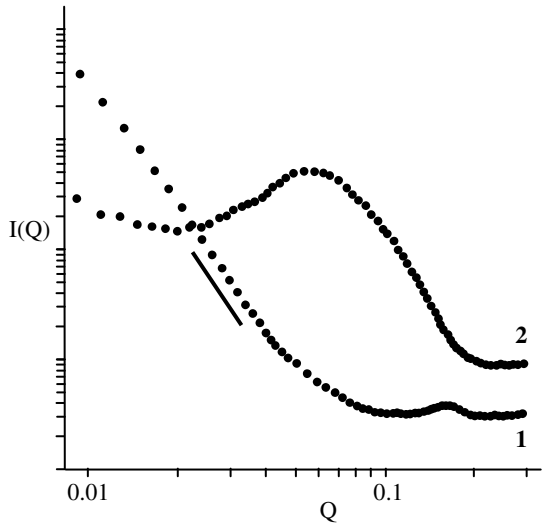

Figure S1. Azymutally averaged scattering intensity from bottom to top of a 1% gel of the APTES salt of myristic acid (1) at room temperature and at 60°C (2). For the sake of clarity, the diffusion patterns were vertically shifted. The slope of Q^{-4} is drawn to guide the eyes.

6) Emulsion formulation:

Emulsions were prepared with 25 vol% n-hexadecane (Sigma Chemicals) as oil phase, and 75 vol% of aqueous phase (lipid dispersion). In all cases a fixed volume (20 mL) of emulsion was prepared in glass tubes with a height of 10 cm, an internal diameter of 2.2 cm and a flat bottom by sonication with a 2 mm diameter probe (Vibracell, 20kHz, 130W, Bioblock Scientific, Illkirch, France). For emulsion stability measurements, the video imaging system was used. A 3CCD color camera (Hamamatsu Photonics France) equipped with a 16 mm television lens (Cosmicar) makes it possible to acquire automatically images of emulsions at predetermined times.

7) Transmission electron microscopy (TEM), Energy-filtered TEM and electron energy loss spectroscopy (EELS):

TEM - A drop of each aqueous dispersion specimen was first placed on a carbon-coated TEM copper grid (Quantifoil, Germany) and let to air-drying. The sample was then negatively stained with uranyl acetate (Merck, Germany). For that, the sample-coated TEM grid was successively placed on a drop of an aqueous solution of uranyl acetate (2 % w/w) and on a drop of distilled water. The grid was then air-dried before introducing them in the electron microscope. The samples were viewed using a JEOL JEM-1230 TEM operating at 80 kV.

EF-TEM and EELS – The EF-TEM images and EELS spectra were acquired from unstained samples using a Gatan GIF-2001 system, including a parallel EELS spectrometer, attached to the JEM-1230 TEM and operated at 120kV with a LaB_6 cathode. The elemental maps were obtained by the three-windows power law method, filtering below the Si specific absorption edges filtered at an energy loss of 100 eV (energy window of 20 eV). EEL spectra were acquired in the diffraction mode using a camera length of 20 cm, a 100 μm spectrometer entry aperture, illumination angles around 1.5 mrad and exposure times between 5 and 30s.

(1) Davis, J., *Biochimica et Biophysica Acta (BBA) - Biomembranes* **1983,** *737*, 117-171.
(2) Seelig, J., *Quart. Rev. Biophys.* **1977,** *10*, 353-418.
(3) Douliez, J.-P., *Langmuir* **2004,** *20*, 1543-1550.
(4) Douliez, J.-P.; Navailles, L.; Nallet, F., *Langmuir* **2006,** *22*, 622-627.
(5) Glatter, O.; Kratky, O., *Academic press, London* **1982,** *3*.